Exciton polaritons in a cylindrical microcavity with an embedded quantum wire

M. A. Kaliteevski, S. Brand, and R. A. Abram
Department of Physics, University of Durham South Road, Durham DH1 3LE, United Kingdom

V. V. Nikolaev
School of Physics, University of Exeter, Stocker Road, Exeter EX4 4QL, United Kingdom

M. V. Maximov and N. N. Ledentsov
Ioffe Physicotechnical Institut of Russian Academy of Science, 26 Polytechnicheskaya, St. Petersburg, Russia

C. M. Sotomayor Torres
Institute of Materials Science and Department of Electrical Engineering, University of Wuppertal, Gauss-Strasse 20, 42097 Wuppertal, Germany

A. V. Kavokin
Université Blaise Pascal Clermont II, Complexe Scientifique des Czeaux, 24 avenue des Landais, 63177 Aubiere, Cedex, France
(Received 29 November 1999)

Exciton-light coupling in cylindrical microcavities containing quantum wires has been treated by means of classical electrodynamics within the nonlocal dielectric response model. A typical anticrossing behavior of quasi-one-dimensional exciton-polariton modes has been obtained, as well as the weak-coupling–strong-coupling threshold. Effects of the nonradiative damping of the exciton resonance in the quantum wire on the optical response of the microcavity structure have been analyzed.

I. INTRODUCTION

One of the major trends of modern semiconductor research is toward the achievement of electron and photon states of low dimensionality.[1] Electrons and holes can be localized in semiconductor heterostructures, such as quantum wells, wires, and dots, which have spatial sizes of several nanometers, and which are comparable with the de Broglie wavelength of an electron. Similarly, photons can be localized by periodic modulation of the refractive index of the medium in different types of microcavities,[2,3] with a feature size of the order of a micrometer or below, and comparable with the wavelength of light.

Quantum wells, providing the confinement of electrons or excitons in only one direction, can be fabricated by different epitaxial techniques. Quantum dots, providing full three-dimensional confinement of excitons, have been obtained by the technique of spontaneous formation during epitaxial growth.[4,5] At present, the most developed method of fabricating quantum wires (QW's), where excitons are localized in two dimensions, is growth on V-grooved substrates,[6] but only QW's parallel to the substrate can be obtained by this technique. A very promising approach to fabricate QW's oriented perpendicularly to the substrate surface is to stack a large number of layers of vertically coupled quantum dots.[7] Due to the strong vertical coupling between the dots, the electron states in such structures are of a quasi-one-dimensional type.

The technology of the fabrication of planar microcavities, where one-dimensional localization of light occurs, is well established, and the interaction of quantum-well excitons and localized photon states in such structures has been the subject of intensive studies in the last decade.[8–10] By providing a substantial enhancement of light-matter interaction, microcavities make possible an experimental investigation of various fundamental effects, such as the propagation of two-dimensional exciton-polaritons,[9] vacuum field Rabi splitting,[11] enhancement of spontaneous emission,[12] etc.

The interaction of quasi-one- and quasi-zero-dimensional photons with excitons has been a subject of considerable interest in the scientific community in the last decade. First, the three-dimensional confinement of photons was achieved in pillar microcavities for certain modes.[13–17] The theory of light-matter interaction in this kind of structure was recently developed.[18] The semiclassical model of light-exciton coupling in gratings of quantum wires was also developed[19] and compared with experimental data on the optical spectroscopy of gratings of quantum wires.[20,21] This approach was extended for a description of the optical spectra of microcavities containing quantum wires.[22] Recently, the two-dimensional localization of light by a cylindrical multilayered structure was demonstrated,[2] and the optical eigenmode structure of such a cylindrical microcavity was analyzed theoretically.[23]

The aim of the present work is to develop a formalism for a description of light-matter interaction in a system with cylindrical symmetry and containing an embedded quantum wire, and to investigate the exciton-polariton state originating from the coupling of a one-dimensional (1D) quantum wire exciton to a 1D photon mode in a cylindrical microcavity. The type of model structure considered is shown in Fig. 1. It has an infinitely long cylindrical microcavity with its axis of symmetry, taken parallel to the z axis, formed by a central cylinder with a radius of the order of the wavelength

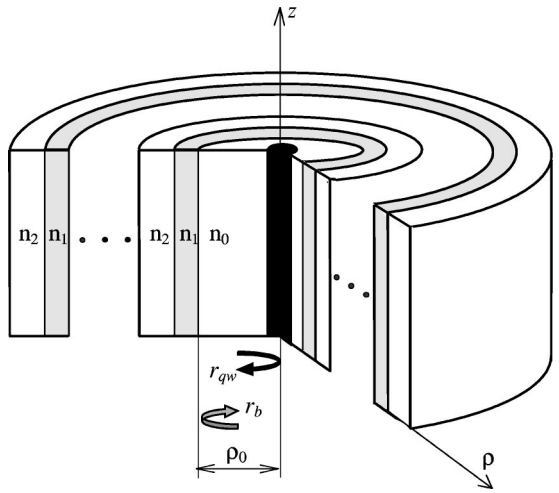

FIG. 1. An illustration of a cylindrical microcavity with quantum wire at its center. A central core of the refractive index n_0 is surrounded by a cylindrical Bragg reflector, constructed from alternate layers of the refractive index n_1 and n_2.

of light, and surrounded by a cylindrical Bragg reflector.[24] A relatively thin cylindrical quantum wire is placed at the center of the structure. Corresponding experimental structures will be susceptible to a degradation of their cavity Q factors due to the out-of-plane scattering assosiated with their finite length. Therefore, the parameters of experimental cylindrical microcavities of this type should be chosen to minimize such light scattering,[2] or some photonic band-gap structure should be used to suppress the scattering.

II. BASIC EQUATIONS

A. Reflection of the cylindrical light wave by a quantum wire

Consider an E-polarized cylindrical wave of a frequency ω incident on a cylindrical quantum wire. E polarization means in this case that the electric-field vector is directed along the axis of the quantum wire.[25] The medium is characterized by a background dielectric constant ϵ. The electromagnetic field of the diverging cylindrical wave has the form

$$E_z = AH_m^{(1)}(k\rho)\exp(im\varphi),$$

$$H_\varphi = i\sqrt{\varepsilon}AH_m^{(1)\prime}(k\rho)\exp(im\varphi), \tag{1}$$

$$H_\rho = (mc/\rho\omega)AH_m^{(1)}(k\rho)\exp(im\varphi),$$

where A is the constant, m is an aztimuthal number, $H_m^{(1)}(k\rho)$ is the Hankel function of the first type, c is the light velocity in vacuum, and $k=\sqrt{\epsilon}(\omega/c)$. The electromagnetic field of the converging cylindrical wave has the form

$$E_z = AH_m^{(2)}(k\rho)\exp(im\varphi),$$

$$H_\varphi = i\sqrt{\varepsilon}AH_m^{(2)\prime}(k\rho)\exp(im\varphi), \tag{1'}$$

$$H_\rho = (mc/\rho\omega)AH_m^{(2)}(k\rho)\exp(im\varphi),$$

where $H_m^{(2)}(k\rho)$ is the Hankel function of the second type. In the following we assume the light wave is propagates in the plane orthogonal to the wire, and consider only the exciton ground state in the wire, which is characterized by zero angular momentum.

The electromagnetic field in the vicinity of the quantum wire is described by Maxwell's equations when the excitonic contribution to the dielectric polarization P_{exc} is taken into account[19]:

$$\Delta_\perp E_z + k^2 E_z = -4\pi\frac{\omega^2}{c^2}P_{exc}(\vec{\rho}). \tag{2}$$

Here

$$P_{exc}(\vec{\rho}) = \int \chi(\omega,\vec{\rho},\vec{\rho}')\vec{E}(\vec{\rho}')d\vec{\rho}' \tag{3}$$

is the nonlocal dielectric susceptibility, whose dependence on the exciton envelope function is given by

$$\chi(\omega,\vec{\rho},\vec{\rho}') = \tilde{\chi}(\omega)\Phi(\vec{\rho})\Phi(\vec{\rho}'), \tag{4}$$

where $\Phi(\vec{\rho})$ is related to the envelope function of the exciton ground state by $\Phi(\vec{\rho})=\sqrt{L}\Psi(\vec{\rho},\vec{\rho})$, and L is the length of the wire.

Substituting formula (5) into Eq. (4), one can rewrite the excitonic polarization as

$$P_{exc}(\vec{\rho}) = \tilde{\chi}(\omega)\Phi(\vec{\rho})\Lambda, \tag{5}$$

where $\Lambda_m = \int\Phi(\vec{\rho})E(\vec{\rho})d\vec{\rho}$ (for details, see Ref. 19). Given the cylindrical symmetry of the exciton ground state, the integral in Eq. (5) is nonzero only in the case of cylindrical light waves having zero angular momentum. Thus in the following we limit the discussion to that situation only. In that case

$$\tilde{\chi}(\omega) = \frac{\varepsilon\omega_{LT}\pi a_B^3}{\tilde{\omega}_{ex}-\omega-i\Gamma}, \tag{6}$$

where $\tilde{\omega}_{ex}$ is the exciton resonance frequency, ω_{LT} is the exciton longitudinal-transverse splitting in the bulk material, a_B is the exciton Bohr radius in the bulk material, and Γ is the exciton nonradiative damping.

The solution of the inhomogeneous Helmholtz equation (2) can be found by the Green-function technique as

$$E(\vec{\rho}) = E_{hom}(\vec{\rho}) + k_0^2\int G(\vec{\rho},\vec{\rho}')P_{exc}(\vec{\rho}')d\vec{\rho}', \tag{7}$$

where $G(\vec{\rho},\vec{\rho}')=i\pi H_0^{(1)}(k|\vec{\rho}-\vec{\rho}'|)$ is the Green function of Eq. (2), and $E_{hom}(\vec{\rho})$ is the solution of the corresponding homogeneous equation. In the empty microcavity the field must be finite at $\rho=0$, which requires that

$$E_{hom} = H_0^{(1)}(k\rho) + H_0^{(2)}(k\rho) = 2J_0(k\rho), \tag{8}$$

where $J_0(k\rho)$ is the zeroth-order Bessel function, and it is assumed that the waves have an amplitude equal to unity.

Substituting Eq. (5) into Eq. (7) gives

$$E(\vec{\rho}) = 2J_0(k\rho) + k_0^2\tilde{\chi}(\omega)\Lambda\int G(\vec{\rho},\vec{\rho}')\Phi(\vec{\rho}')d\vec{\rho}'. \tag{9}$$

Then, multiplying both sides of Eq. (9) by $\Phi(\vec{\rho})$ and integrating over $\vec{\rho}$ results in the linear equation for Λ,

$$\Lambda = 2\Lambda_{hom} + k_0^2 \tilde{\chi}(\omega)\Lambda I, \tag{10}$$

where $\Lambda_{hom} = \int J_0(k\vec{\rho})\Phi(\vec{\rho})d\vec{\rho}$ and

$$I = \int G(\vec{\rho},\vec{\rho}')\Phi(\vec{\rho}')\Phi(\vec{\rho})d\vec{\rho}'d\vec{\rho}.$$

In order to find the value of the integral $\int G(\vec{\rho},\vec{\rho}')\Phi(\vec{\rho}')d\vec{\rho}'$, it is convenient to represent the Green function in the form[26]

$$G(\vec{\rho},\vec{\rho}') = i\pi \begin{cases} \sum_{n=-\infty}^{+\infty} H_n^{(1)}(k\rho)J_n(k\rho')\exp[in(\varphi-\varphi')], & \rho > \rho' \\ \sum_{n=-\infty}^{+\infty} H_n^{(1)}(k\rho')J_n(k\rho)\exp[in(\varphi-\varphi')], & \rho < \rho'. \end{cases} \tag{11}$$

From the above-mentioned symmetry arguments, only those terms in the sums in Eq. (11) which have $n=0$ give nonzero contribution to the value of integral. Thus one can write

$$\begin{aligned} &\int H_0^{(1)}(k|\vec{\rho}-\vec{\rho}'|)\Phi(\vec{\rho}')d\vec{\rho}' \\ &= 2\pi\int_0^{\infty} \begin{pmatrix} H_0^{(1)}(k\rho)J_0(k\rho'), & \rho > \rho' \\ H_0^{(1)}(k\rho')J_0(k\rho), & \rho' > \rho \end{pmatrix} \Phi(\rho')\rho' d\rho' \\ &= 2\pi\Bigg[J_0(k\rho)\int_0^{\infty} J_0(k\rho')\Phi(\rho')\rho' d\rho' \\ &\quad + iY_0(k\rho)\int_0^{\rho} J_0(k\rho')\Phi(\rho')\rho' d\rho' \\ &\quad + iJ_0(k\rho)\int_{\rho}^{\infty} Y_0(k\rho')\Phi(\rho')\rho' d\rho' \Bigg]. \end{aligned} \tag{12}$$

The integral in the first term on the right of Eq. (12) is just Λ_{hom}. The wave function $\Phi(\vec{\rho})$ decays exponentially on the length scale of a_B outside the quantum wire, so that, for large ρ (compared to a_B),

$$\int G(\vec{\rho},\vec{\rho}')\Phi(\vec{\rho}')d\vec{\rho}' = i\pi\Lambda_{hom}H_0^{(1)}(k\rho). \tag{13}$$

Using relation (13), Eq. (9) can be rewritten in the form

$$E(\vec{\rho}) = H_0^{(2)}(k\rho) + [1 + i2\pi k_0^2\tilde{\chi}(\omega)\Lambda\Lambda_{hom}]H_0^{(1)}(k\rho). \tag{14}$$

We define the reflection coefficient of the wire as the ratio of the amplitudes of the diverging and converging waves [i.e., the ratio of the coefficients of $H_0^{(1)}(k\rho)$ and $H_0^{(2)}(k\rho)$ in Eq. (14)]. Thus we obtain

$$r_{QW} = 1 + i\pi k_0^2\tilde{\chi}(\omega)\Lambda\Lambda_{hom}. \tag{15}$$

Substituting the value of Λ from Eq. (10) into Eq. (15) gives

$$r_{QW} = 1 + \frac{2\pi i k_0^2\tilde{\chi}(\omega)\Lambda_{hom}^2}{1 - k_0^2\tilde{\chi}(\omega)I}. \tag{16}$$

Then, multiplying the numerator and denominator of ratio (16) by $\tilde{\omega}_{ex} - \omega - i\Gamma$, we obtain the reflection coefficient in the form

$$r_{QW} = 1 + \frac{i\gamma}{\omega_{ex} - \omega - i(\Gamma + \Gamma_0)}, \tag{17}$$

where

$$\gamma = 2\pi^2 k_{ex}^2 \omega_{LT} a_B^3 \Lambda_{hom}^2, \tag{18}$$

$$\omega_{ex} = \tilde{\omega}_{ex} - \pi k_{ex}^2 \omega_{LT} a_B^3 \,\mathrm{Re}(I), \tag{19}$$

$$\Gamma_0 = \pi k_{ex}^2 \omega_{LT} a_B^3 \,\mathrm{Im}(I), \tag{20}$$

and $k_{ex} = \sqrt{\varepsilon_B}(\tilde{\omega}_{ex}/c)$.

Using Eq. (11), the integral I can be represented in the form

$$\begin{aligned} I &= i\pi \int H_0^{(1)}(k|\vec{\rho}-\vec{\rho}'|)\Phi(\rho')\Phi(\rho)d\vec{\rho}'d\vec{\rho} \\ &= 4\pi^3 i \int_0^{\infty} J_0(k\rho)\Phi(\rho)\rho\, d\rho \int_0^{\infty} J_0(k\rho')\Phi(\rho')\rho' d\rho' \\ &\quad - 4\pi^3 \int_0^{\infty} Y_0(k\rho)\Phi(\rho)\left[\int_0^{\rho} J_0(k\rho')\Phi(\rho')\rho' d\rho'\right]\rho\, d\rho \\ &\quad - 4\pi^3 \int_0^{\infty} J_0(k\rho)\Phi(\rho)\left[\int_{\rho}^{\infty} Y_0(k\rho')\Phi(\rho')\rho' d\rho'\right]\rho\, d\rho, \end{aligned} \tag{21}$$

from which it follows that $\mathrm{Im}(I) = \pi\Lambda_{hom}^2$ and $\gamma = 2\Gamma_0$.

Finally, we obtain the reflection coefficient of the wire:

$$r_{QW} = 1 + \frac{2i\Gamma_0}{\omega_{ex} - \omega - i(\Gamma + \Gamma_0)}. \tag{22}$$

In a similar fashion, the reflection coefficients of converging cylindrical electromagnetic wave, characterized by non-zero azimuthal number can be obtained.

B. Eigenmodes of a cylindrical microcavity with an embedded quantum wire

An electromagnetic field in a central cylinder containing a quantum wire located at the symmetry axis has the form

$$E(\rho) = H_0^{(2)}(k\rho) + r_{QW}H_0^{(1)}(k\rho), \tag{23}$$

and can be represented as two-dimensional vector $[H_0^{(2)}(k\rho), r_{QW}H_0^{(1)}(k\rho)]$, whose components are the magnitudes of the converging and diverging waves.

At the boundary of the central cylinder, which is at radius ρ_0, the ratio of the amplitudes of the converging and diverging waves is given by the reflection coefficient r_b of the

cylindrical Bragg mirror, which provides the optical confinement in the structure, and can represented as $C(r_b,1)$, where C is the constant.

The equation defining the frequencies of the eigenmodes of the cylindrical microcavity with an embedded quantum wire can be obtained by equating the two vectors defined above, to give

$$H_0^{(2)}(k\rho_0)=r_b r_{QW} H_0^{(1)}(k\rho_0). \tag{24}$$

In the case of negligible decay of light in the structure, Eq. (24) can be reduced to

$$\arg[H_0^{(1)}(k\rho_0)] - \arg[H_0^{(2)}(k\rho_0)]+\arg(r_b)+\arg(r_{QW})=2\pi j. \tag{25}$$

Further simplifications can be achieved by use of the approximate relations $\arg[H_0^{(1)}(k\rho_0)]\cong k\rho_0-\pi/4$ and $\arg(H_0^{(2)}(k\rho_0))\cong -k\rho_0+\pi/4$, which will be valid if the internal radius of the cavity exceeds the wavelength of light. The phase of the reflection coefficient of the Bragg mirror at the Bragg frequency can be approximated by the simplified expression,[27] which is also valid in the cylindrical case,[24]

$$\arg(r_b)=b\frac{\omega-\omega_b}{\omega_b}, \tag{26}$$

where $b=\pi n_1 n_2/\sqrt{\varepsilon}(n_2-n_1)$, and n_1 and n_1 are the refractive indices of the layers forming the mirror.

The reflection coefficient of the quantum wire can be represented in form

$$r_{QW}=\frac{(\omega_{ex}-\omega)^2+(\Gamma^2-\Gamma_0^2)+i2\Gamma_0(\omega_{ex}-\omega)}{(\omega_{ex}-\omega)^2+(\Gamma+\Gamma_0)^2} \tag{27}$$

The phase can be found as

$$\arg(r_{QW})=\arctan\left(\frac{2\Gamma_0(\omega_{ex}-\omega)}{(\omega_{ex}-\omega)^2+(\Gamma+\Gamma_0)^2}\right). \tag{28}$$

Let us now assume that the exciton-polariton eigenmode frequencies are significantly different from the frequency of the exciton resonance ω_{ex} (which is the case in planar microcavities in the strong coupling regime), so that $(\Gamma+\Gamma_0)\ll|\omega_{ex}-\omega_{em}|$ where ω_{em} is the eigenmode frequency of the structure. Then we find

$$\arg(r_{QW})\cong\frac{2\Gamma_0}{(\omega_{ex}-\omega_{em})}. \tag{29}$$

Using relations (26) and (29) one can represent Eq. (25) in the form

$$2\sqrt{\varepsilon}\,\frac{\omega_{em}}{c}\rho_0+b\frac{\omega_{ex}-\omega_b}{\omega_b}+\frac{2\Gamma_0}{(\omega_{ex}-\omega_{em})}=2\pi j+\pi/2. \tag{30}$$

The frequency interval between optical eigenmode frequencies in the empty cavity,[23]

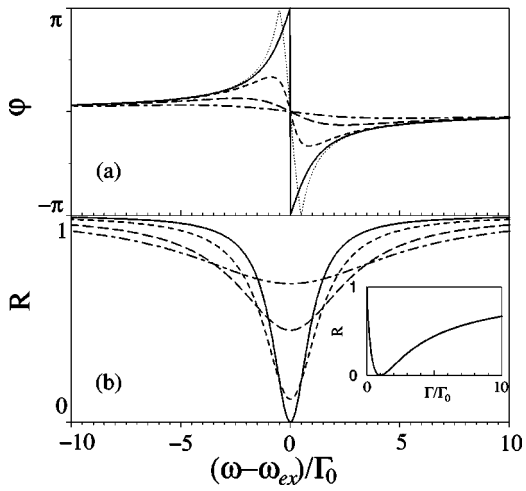

FIG. 2. Spectral dependence of the phase (a) and the square modulus of the amplitude reflection coefficient (b) of a converging E-polarized cylindrical wave incident on the quantum wire, and characterized by azimuthal number $m=0$. Curves for different values of Γ are shown: dotted line, $\Gamma=0$; solid line, $\Gamma=\Gamma_0$; short-dashed line, $\Gamma=2\Gamma_0$; long-dashed line, $\Gamma=5\Gamma_0$; and dash-dotted line, $\Gamma=10\Gamma_0$. The inset shows the power reflection coefficient at the resonant frequency vs the value of non radiative damping Γ.

$$\Delta\omega_j=\frac{2\pi\omega_b}{2\sqrt{\varepsilon}\rho_0\omega_b/c+b}, \tag{31}$$

is quite large compared to the typical Rabi-splitting values,[9] and we may consider the exciton coupling with a single optical mode. This allows us to rewrite Eq. (30) in the simple form

$$(\omega_{em}-\omega_{0j})(\omega_{em}-\omega_{ex})=(\Delta/2)^2, \tag{32}$$

where Δ is the Rabi splitting given by

$$\Delta=2\sqrt{\frac{2\Gamma_0\omega_b}{b+2\sqrt{\varepsilon}\rho_0\omega_b/c}}, \tag{33}$$

and ω_{0j} is the optical mode frequency closest to the exciton resonance:

$$\omega_{0j}=\frac{2\pi j+\pi/2+b}{2\sqrt{\varepsilon}\rho_0/c+b/\omega_b}. \tag{34}$$

Equation (33) has a different form of denominator from planar case, which can be explained by the different symmetry of the system. The phase changes of light during a ''round trip'' in the cavity is different in the case of cylindrical microcavity. The following estimates are finally obtained for the exciton-polariton eigenmode frequencies:

$$\omega_{em}=\frac{\omega_{0j}+\omega_{ex}}{2}\pm\frac{1}{2}\sqrt{(\omega_{0j}-\omega_{ex})^2+4\Delta^2}. \tag{35}$$

III. RESULTS AND DISCUSSION

Figure 2 shows the spectral dependence of the phase and the squared modulus of the amplitude reflection coefficient of the incident cylindrical converging wave for different val-

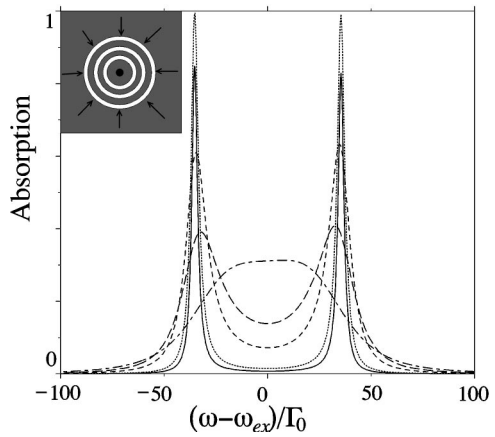

FIG. 3. Absorption spectrum of a cylindrical microcavity with the quantum wire for a converging *E*-polarized cylindrical wave with azimuthal number $m=0$. Different values of are shown: solid line, $\Gamma=\Gamma_0$; dotted line, $\Gamma=2\Gamma_0$; short-dashed line, $\Gamma=10\Gamma_0$; long-dashed line, $\Gamma=20\Gamma_0$; and dash-dotted line, $\Gamma=50\Gamma_0$. The inset shows a schematic view of the cross section of the structure: a central core with the quantum wire in the center, surrounded by cylindrical Bragg reflector. The refractive indices of the central core, outer media, and the two layers of the Bragg reflector, shown in gray, are equal to 3.0, while refractive index of the three white layers are equal to 1.0. The thicknesses of the layers of the reflector are a quarter of the wavelength corresponding to the exciton resonance frequency ω_{ex}. The radius of the central core is chosen to provide an exact tuning of the optical eigenmode frequency ω_{0j} to the exciton resonance frequency and satisfies the relation $\rho_0\omega_{ex}/2\pi c=0.37015$.

ues of Γ. Note that in the case $\Gamma=0$, the magnitude of the reflection coefficient is equal to unity, while the phase changes strongly in the vicinity of the exciton resonance. The latter effect can be easily understood if one takes into account that it describes the dissipation of energy, and in the case of a cylindrical wire and $\Gamma=0$, the entire energy of the converging wave must reappear in the diverging wave. This is because any energy in the converging wave that is not absorbed reaches the line $\rho=0$, and then contributes to the wave diverging from there. For $\Gamma=\Gamma_0$ the reflection spectrum exhibits a dip that becomes zero at its minimum. With a further increase of Γ, the dips in the spectra become shallower and broader. When the frequency of the incident wave is tuned to the exciton resonance frequency, the amplitude reflection coefficient can be represented in the form $r_{QW}=(\Gamma-\Gamma_0)/(\Gamma+\Gamma_0)$ (see the inset in Fig. 2). The total absorption of the incident radiation is a feature of the cylindrical system which is absent in planar microcavities.

Figure 3 presents absorption spectra of the cylindrical microcavity with an embedded quantum wire shown in the figure inset. The model microcavity consists of a central core having a refractive index of 3.0, surrounded by a cylindrical Bragg reflector, as described in the figure caption. The parameters of the microcavity are chosen to tune one of the optical eigenmodes of the cavity without the quantum wire to the wire exciton frequency. The value of the radiative damping is $\Gamma_0=0.0001\omega_{ex}$, which is typical of the relative values of the oscillator strength and exciton resonance frequency for real quantum wires.

The spectral positions of the absorption peaks correspond

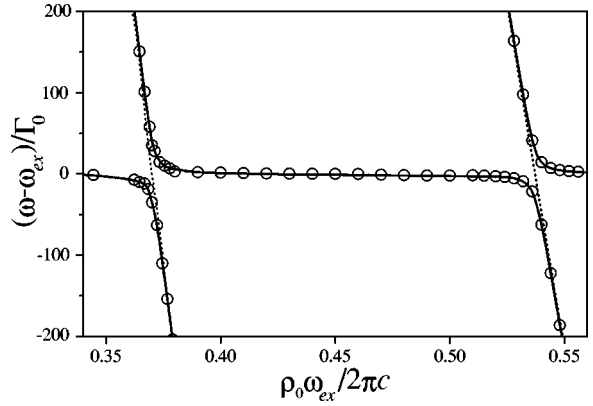

FIG. 4. Dependence of the eigenmode frequencies of the cylindrical microcavity with quantum wire on the central cylinder radius. The dotted lines show the optical eigenmodes of a microcavity without the quantum wire. The solid lines show the dependences, obtained using Eq. (25). The circles show the positions of the absorption peaks.

to the eigenmode frequencies in the system. If the exciton broadening is much smaller than the Rabi splitting Δ, the absorption spectra exhibit two peaks with center frequencies that are quite insensitive to the value of the nonradiative damping factor Γ, but do show significant variations in their linewidths and amplitudes. The coexistence of two peaks in the spectra is evidence of the strong-coupling regime.[8] However, when Γ is comparable to Δ, the weak-coupling regime occurs, and the two peaks in the absorption spectra merge into one broad peak, centered at the frequency of the exciton resonance. These properties are analogous to those for the interaction of photon and exciton modes in a planar microcavity containing a quantum well.[1]

The dependence of the optical eigenmode frequency on the central cylinder radius ρ_0 of an empty cylindrical micro-

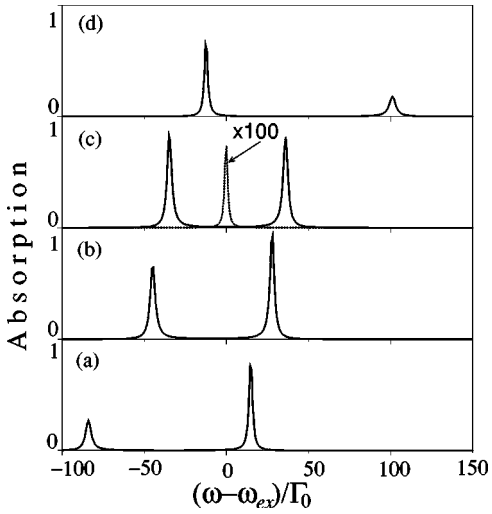

FIG. 5. Absorption spectra for different values of the central core radius. The solid lines correspond to the cases (a) $\rho_0\omega_{ex}/2\pi c=0.3735$, (b) $\rho_0\omega_{ex}/2\pi c=0.3713$, (c) $\rho_0\omega_{ex}/2\pi c=0.37015$, and (d) $\rho_0\omega_{ex}/2\pi c=0.3668$, which are all close to the anticrossing feature in Fig. 4. The dotted line in (c) shows the absorption spectrum for $\rho_0\omega_{ex}/2\pi c=0.465$, corresponding to an essentially uncoupled exciton.

cavity exhibits a series of branches, as shown in Fig. 4. In each branch, the frequency increases with decreasing radius ρ_0. The splitting between two neighboring branches characterized by the same azimuthal number is given by formula (31). By changing the radius ρ_0 it is possible to tune the optical eigenmode frequency ω_{0j} into resonance with the quantum wire exciton. The coupling of a photon and an exciton state leads to the anticrossing behavior seen in the figure. The optical eigenmode branch crosses the exciton resonance frequency ω_{ex} when the radius ρ_0 approaches the value satisfying the relation $\rho_0\omega_{ex}/2\pi c = 0.37$. Figure 4 also shows another anticrossing at $\rho_0\omega_{ex}/2\pi c \approx 0.54$, where the exciton state couples with another optical eigenmode.

The change in shape of the absorption spectrum with variation of the radius ρ_0 around the value corresponding to the first anticrossing is illustrated by the solid lines in Fig. 5. When the detuning of the exciton and the photon modes is strong there are two distinct peaks in the absorption spectra, and the frequencies of these two peaks nearly correspond to the uncoupled exciton and photon states [Fig. 5(a)]. Tuning the optical mode to the exciton frequency leads to the shift of both resonances which exhibits identical shape in the case of precise tuning [Fig. 5(c)]. The splitting between the peaks in this case is almost identical to the value of the vacuum-field Rabi splitting Δ given by Eq. (33). The dotted curve in Fig. 5(c), which corresponds to the value of ρ_0 well removed from the anticrossing, illustrates how much weaker the excitonic absorption is when the exciton and optical modes are essentially uncoupled.

IV. CONCLUSION

Exciton-light interactions in a system of cylindrical symmetry have been theoretically analyzed using the nonlocal dielectric response model. An interesting peculiarity of the cylindrical system is that a converging cylindrical electrodynamic wave can be fully absorbed by quantum wire exciton. An equation for the energies of the polariton states originating from the optical eigenmode of the cylindrical microcavity and the quantum wire exciton has been obtained, and simplified approximate formulas have also been derived. The state energies exist on a series of anticrossing branches when plotted as a function of the inner radius of the microcavity. The transition between weak- and strong-coupling regimes has also been illustrated, and is similar to the case of a quantum well in a planar microcavity.

ACKNOWLEDGMENTS

The work was partly funded by an EPRSC research grant, and partly by RFBR and NATO Linkage HTEC Grant No. 974673.

[1] *Confined Exciton and Photons: New Physics and Devices*, edited by E. Burstein and C. Weisbush (Plenum, New York, 1994).

[2] D. Liballoy, H. Benisty, C. Weisbouch, T.F. Kraus, C.J. Smith, R. Houdre, and U. Oesterle, Appl. Phys. Lett. **73**, 1314 (1998).

[3] C.J.M. Smith, R. M De la Rue, H. Benisty, U. Oesterle, T.F. Krauss, D. Labilloy, C. Weisbuch, and R. Houdre, IEE Proc.: Optoelectron. **145**, 373 (1998).

[4] M. Grundmann, J. Christen, N.N. Ledentsov, J. Bohrer, D. Bimberg, S.S. Ruvimov, P. Werner, U. Richter, U. Gosele, J. Heydenreich, V.M. Ustinov, A. Yu. Egorov, A.E. Zhukov, P.S. Kop'ev, and Zh.I. Alferov, Phys. Rev. Lett. **74**, 4043 (1995).

[5] J.-Y. Marzin, J.-M. Gerard, A. Izrael, D. Barrier, and G. Bastard, Phys. Rev. Lett. **73**, 716 (1994).

[6] Eli Kapone, in *Optical Properties of Low Dimensional Semiconductors*, Vol. 344 of *Nato Advanced Study Institute, Series E: Applied Science*, edited by G. Abstreiter, A. Aydinli, and J.-P. Leburton, (Kluwer, Dordrecht, 1997), pp. 99–125.

[7] N.N. Ledentsov, V.A. Shchukin, M. Grundmann, N. Kirstaedter, J. Bohrer, O. Schmidt, D. Bimberg, V.M. Ustinov, A.Y. Egorov, A.E. Zhukov, P.S. Kop'ev, S.V. Zaitsev, N.Y. Gondecv, Zh.I. Alferov, A.O. Kosogov, S.S. Ruvimov, P. Werner, U. Gosele, and J. Heydenreich, Phys. Rev. B **54**, 8743 (1996).

[8] C. Weisbuch, M. Hishioka, A. Ishikava, and Y. Arakawa, Phys. Rev. Lett. **69**, 3314 (1992).

[9] G. Panzarini, L.C. Andreani, A. Armitage, D. Baxter, M.S. Skolnick, V.N. Astratov, J.S. Roberts, A.V. Kavokin, M.R. Vladimirova, and M.A. Kaliteevski, Phys. Rev. B **59**, 5082 (1999).

[10] D. Baxter, M.S. Skolnick, A. Armitage, V.N. Astratov, D.M. Whittaker, T.A. Fisher, J.S. Roberts, D.J. Mowbray, and M.A. Kaliteevski, Phys. Rev. B **56**, 10 032 (1997).

[11] J. Tignon, P. Voisin, C. De La Lande, M. Voos, R. Houdre, U. Osterle, and R.P. Stanley, Phys. Rev. Lett. **74**, 3967 (1995).

[12] E.M. Purcell, Phys. Rev. **69**, 681 (1946).

[13] J.M. Gerard, D. Barrier, J.Y. Marzin, R. Kuszelewicz, L. Manin, E. Costard, V. Thierry-Mieg, and T. Rivera, Appl. Phys. Lett. **69**, 449 (1996).

[14] B. Ohnesorge, M. Bayer, A. Forchel, J.P. Reithmaier, N.A. Gippius, and S.G. Tikhodeev, Phys. Rev. B **56**, R4367 (1997).

[15] J.M. Gerard, B. Sermage, B. Gayral, B. Legrand, E. Costard, and V. Thierry-Mieg, Phys. Rev. Lett. **81**, 1110 (1998).

[16] J. Bloch, F. Bouf, J.M. Gerard, B. Legrand, J.Y. Marzin, R. Planel, V. Thierry-Mieg, and E. Costard, Photonics Spectra **16**, 915 (1998).

[17] T. Gutbrod, M. Bayer, A. Forchel, J.P. Reithmaier, J.P. Reinecke, S. Rudin, and P.A. Knipp, Phys. Rev. B **57**, 9950 (1998).

[18] L.C. Andreani, G. Panzarini, and J.M. Gerard, Phys. Rev. B **60**, 13 276 (1999).

[19] E.L. Ivchenko, A.V. Kavokin, Fiz. Tverd. Tela (Leningrad) **34**, 1815 (1992) [Sov. Phys. Solid State **34**, 1815 (1992)].

[20] E.L. Ivchenko, A.V. Kavokin, V.P. Kochereshko, P.S. Kop'ev, and N.N. Ledentsov, Superlattices Microstruct. **12**, 317 (1992).

[21] V.P. Kochereshko, E.L. Ivchenko, A.V. Kavokin, P.S. Kop'ev, N.N. Ledentsov, J. Phys. (Paris) Colloq. **3**, CS-363 (1993).

[22] A.V. Kavokin, M.A. Kaliteevski, and M.R. Vladimirova, Phys. Rev. B **54**, 1490 (1996).

[23] M.A. Kaliteevski, R.A. Abram, and V.V. Nikolaev, J. Mod. Opt. **47**, 677 (2000).

[24] M.A. Kaliteevski, R.A. Abram, V.V. Nikolaev, and G.S. Sokolovski, J. Mod. Opt. **46**, 875 (1999).

[25] This polarization of light corresponds to the polarization obtained

experimentally from the photoluminescence of a large stack of vertically coupled quantum dots. For details, see P. Yu, W. Langbein, K. Leosson, J.M. Hvam, N.N. Ledentsov, D. Bimberg, V.M. Ustinov, A. Yu. Egorov, A.E. Zhukov, A.F. Tsatsul'nikov, and Yu.G. Musikhin, Phys. Rev. B **60**, 16 680 (1999).

[26] I.S. Gradshteyn and I.M. Ryzhik, *Tables of Integral, Series and Products* (Academic Press, London, 1980), p. 979.

[27] E.L. Ivchenko, M.A. Kaliteevski, A.V. Kavokin, and A.I. Nesvizhskii, J. Opt. Soc. Am. B **13**, 1061 (1996).